

Acid Experimental Evolution of the Extremely Halophilic Archaeon Halobacterium sp. NRC-1 Selects Mutations Affecting Arginine Transport and Catabolism

Karina S Kunka

Kenyon College

Jessie M Griffith

Kenyon College

Chase Holdener

Kenyon College

Katarina M Bischof

Kenyon College

Haofan Li

Kenyon College

Priya DasSarma

University of Maryland School of Medicine

Shiladitya DasSarma

University of Maryland School of Medicine

Joan L Slonczewski (✉ slonczewski@kenyon.edu)

Kenyon College

Research article

Keywords: Halobacterium sp. NRC-1, experimental evolution, archaeon

Posted Date: November 7th, 2019

DOI: <https://doi.org/10.21203/rs.2.16925/v1>

License:  This work is licensed under a Creative Commons Attribution 4.0 International License.

[Read Full License](#)

1
2
3
4
5
6
7
8
9
10
11
12
13
14
15
16

Acid Experimental Evolution of the Extremely Halophilic Archaeon *Halobacterium* sp.

NRC-1 Selects Mutations Affecting Arginine Transport and Catabolism

by

Karina S. Kunka,^a Jessie M. Griffith,^a Chase Holdener,^a Katarina M. Bischof,^a Haofan Li,^a Priya
DasSarma,^b Shiladitya DasSarma,^b and Joan L. Slonczewski^{a#}

^aDepartment of Biology, Kenyon College, Gambier, Ohio, USA.

^bInstitute of Marine and Environmental Technology, Department of Microbiology and
Immunology, University of Maryland School of Medicine, Baltimore, Maryland, USA

[#]Corresponding Author:

Joan L. Slonczewski, slonczewski@kenyon.edu

Department of Biology, Kenyon College, Gambier, Ohio, USA

17 ABSTRACT

18 **Background**

19 *Halobacterium* sp. NRC-1 (NRC-1) is an extremely halophilic archaeon that is adapted to
20 multiple stressors such as UV, ionizing radiation and arsenic exposure. We conducted
21 experimental evolution of NRC-1 under acid stress. NRC-1 was serially cultured in CM+
22 medium modified by four conditions: optimal pH (pH 7.5), acid stress (pH 6.3), iron amendment
23 (600 μ M ferrous sulfate, pH 7.5), and acid plus iron (pH 6.3, with 600 μ M ferrous sulfate). For
24 each condition, four independent lineages of evolving populations were propagated. After 500
25 generations, 16 clones were isolated for phenotypic characterization and genomic sequencing.

26 **Results**

27 Genome sequences of all 16 clones revealed 378 mutations, of which 90% were haloarchaeal
28 insertion sequences (ISH) and ISH-mediated large deletions. This proportion of ISH events in
29 NRC-1 was five-fold greater than that reported for comparable evolution of *E. coli*. One acid-
30 evolved clone had increased fitness compared to the ancestral strain when cultured at low pH.
31 Seven of eight acid-evolved clones had a mutation within or upstream of *arcD*, which encodes an
32 arginine-ornithine antiporter; no non-acid adapted strains had *arcD* mutations. Mutations also
33 affected the *arcR* regulator of arginine catabolism, which protects bacteria from acid stress by
34 release of ammonia. Two acid-adapted strains shared a common mutation in *bop*, which encodes
35 the bacteriorhodopsin light-driven proton pump. Unrelated to pH, one NRC-1 minichromosome
36 (megaplasmid) pNRC100 had increased copy number, and we observed several mutations that
37 eliminate gas vesicles and arsenic resistance. Thus, in the haloarchaeon NRC-1, as in bacteria,
38 pH adaptation was associated with genes involved in arginine catabolism and proton transport.

39 **Conclusions**

40 Our study is among the first to report experimental evolution with multiple resequenced genomes

41 of an archaeon. Haloarchaea are polyextremophiles capable of growth under environmental
42 conditions such as concentrated NaCl and desiccation, but little is known about pH stress.
43 *Halobacterium* sp. NRC-1 (NRC-1) is considered a model organism for the feasibility of
44 microbial life in iron-rich brine on Mars. Interesting parallels appear between the molecular basis
45 of pH adaptation in NRC-1 and in bacteria, particularly the acid-responsive arginine-ornithine
46 system found in oral streptococci.
47

48 INTRODUCTION

49
50 *Halobacterium* sp. NRC-1 (NRC-1) is a polyextremophile that grows optimally at NaCl
51 concentrations in excess of 4 molar (1). A genetically tractable model microbe (2), it was the first
52 halophilic Archaeon with a fully sequenced genome (3). Besides high salt, NRC-1 is capable of
53 surviving: high doses of ionizing radiation and dessication (4), UV radiation (5), temperature
54 extremes (6), and toxic ions such as arsenite (7). These traits have made NRC-1 a model for
55 studying the possibility of life outside Earth under conditions such as the stratosphere (8,9) or on
56 Mars (10–12).

57 Water on Mars contains high concentrations of salt, as well as acid and iron (13). The
58 Mars Exploration Rover Opportunity discovered substantial deposits of an iron hydrous sulfate
59 mineral known as jarosite [$\text{KFe}^{3+}_3(\text{OH})_6(\text{SO}_4)_2$] which forms in acidic and iron-rich aqueous
60 environments. On earth such conditions occur in acid mine drainage and near volcanic vents.
61 Opportunity's discovery of jarosite on Mars was evidence of acidic, liquid water and an
62 oxidizing atmosphere in the Martian past (13,14). Occuring together, acid and metals can
63 amplify the stress associated with each condition (15). Thus, it is of interest to investigate how a
64 neutralophilic halophile such as NRC-1 (16) might adapt to conditions of acid and high iron.

65 An informative approach to examine the genomic basis of stress response is experimental
66 laboratory evolution (17–23). Experimental evolution of bacteria reveals changes in phenotype
67 and genotype in response to specific stressors in a controlled environment, such as carbon source
68 limitation or extreme pH. In bacterial adaptation to various kinds of pH stress, we find a
69 recurring pattern that dominant responses to short-term stress actually decrease fitness over many
70 generations of long-term exposure. For example, amino-acid transport and catabolism play
71 important roles in extreme-acid survival of *Escherichia coli* (24,25). However, 2,000 generations

72 of *E. coli* evolution at pH 4.8 select for loss of three acid-inducible amino-acid decarboxylase
73 systems, including arginine decarboxylase (21). As a membrane-permeant acid, benzoic acid
74 induces glutamate decarboxylase and drug resistance regulons, yet these systems are lost or
75 downregulated during experimental evolution (26),(20). At high external pH, *E. coli* survival
76 requires the stress sigma factor RpoS; however, generations of growth at high pH select against
77 RpoS expression and activity (27). It is therefore of interest to investigate whether similar
78 patterns of reversal occur in archaea.

79 Relatively few experimental evolution studies have been reported in archaea. In NRC-1,
80 serial application of lethal doses of ionizing radiation selected more resistant mutants that had
81 increased expression of a single-strand DNA binding protein (28). In the thermoacidophile
82 *Sulfolobus solfataricus*, serial passage in extreme acid yielded strains that grow below pH 1 (29).
83 These strains showed mutations in amino acid transporters, as well as upregulation of membrane
84 biosynthesis and oxidative stress response. In *Metallosphaera sedula*, serial passage led to a pH
85 0.9-adapted strain with four mutations, one of which is an amino-acid/polyamine transporter
86 (30). These findings are intriguing, given the role of amino-acid transport and catabolism in
87 extreme-acid survival of bacteria (24,25). For example, arginine transport and catabolism, which
88 yields CO₂ plus two ammonium ions, is a prominent response to acid stress of oral streptococci
89 (31),(32).

90

91 Archaea employ various processes that involve proton transport via primary pumps and
92 antiporters (24,33,34). *Halobacterium* strains possess the light-driven proton pump
93 bacteriorhodopsin (*bop*) that generates proton motive force (PMF) (35,36) as well as several
94 sodium-proton antiporters, which export sodium in exchange for protons (6).

95 We conducted experimental evolution of NRC-1 under conditions of low pH (pH 6.5-6.3)
96 and at optimal pH for growth (pH 7.5), with high iron versus low iron concentration. The NRC-1
97 genome includes a main chromosome and two minichromosomes or megaplasmids (3,37) . It
98 accumulates frequent IS mutations (38,39) which may mediate rapid adaptations to
99 environmental stress. Our study of experimental evolution in a haloarchaeon assesses which
100 mutations contribute to archaeal evolution in acid stress. Here we describe analysis of phenotypic
101 changes across evolved clones from each population, and then use genomic analysis to identify
102 potential underlying mutational bases of these phenotypic responses to selection. Genome
103 analysis of 16 clones revealed a remarkable proportion of events mediated by insertion
104 sequences (ISH). In acid-adapted strains, we found a high frequency of mutations in the arginine-
105 ornithine antiporter *arcD* (40) and in the associated *arcR* arginine catabolism regulator (41).

106 RESULTS

107

108 **Experimental evolution under conditions of acid and iron stress.**

109 Serial culture of evolving populations was conducted as described under Methods (Additional
110 File 1, Fig. S1). Populations of NRC-1 were founded from a single clone and cultured in
111 modified CM⁺ medium (2,3) with appropriate buffers to maintain pH. Each population was
112 diluted 500-fold every four days (approximately 9 generations). Four independent populations
113 were maintained for each condition: the optimal growth condition, pH 7.5 (designation M); acid
114 stress, initially pH 6.5, later pH 6.3 (designated J); iron amendment, pH 7.5 with 600 μ M ferrous
115 sulfate (designated S); and acid with iron amendment (designated K) for a total of 16
116 experimental populations. Populations evolved under acid stress were cultured at an initial pH of
117 6.5, which was then lowered to 6.3 at generation 250, as the populations adapted.

118 After all populations reached 500 doublings, two clones were isolated from each
119 population by three rounds of streaking on CM⁺ agar for a total of 32 evolved clones. Genomic
120 DNA was extracted from 16 of these clones, and from the founder stock of NRC-1. DNA
121 samples were sequenced by Illumina MiSeq, and mutations were identified by comparison of the
122 “evolved strain” sequences to that of the NRC-1 ancestral stock, assembled on the reference
123 genome (3) using the *breseq* pipeline (42–44). The strains we characterized are listed in **Table 1**.

124

125 **Mutations in the genomes from evolving populations.**

126 The genomes of the 16 clones were compared to those of the NRC-1 ancestor which we
127 resequenced from our lab stock (**Tables S1, S2, S3**). The genome of our NRC-1 stock was also
128 compared to that of the NCBI reference sequence *Halobacterium* sp. NRC-1 (3) as shown in
129 Additional File 1, **Table S4**. A small number of positions differed from that of the reference.

130 Some of these differences are consistent with those of later sequence reports (45,46). The
131 sequences differences shown in **Table S4** were excluded in our analysis of the evolved clones.

132 The genomes of the evolved clones had a total of 378 mutations, of which 349 were
133 unique to one strain at the base-pair level. Representative mutations of interest are summarized
134 in **Table 2**. Mutation frequencies were compared for the main replicon and minichromosomes. In
135 total across all resequenced genomes there were 120 mutations in minichromosome pNRC100,
136 and 171 mutations on minichromosome pNRC200. pNRC100 is about 10% as long as the main
137 chromosome, and pNRC200 is about 20% as long; thus, the two minichromosomes had a
138 mutation frequency more than ten-fold greater than that of the main chromosome, a finding
139 consistent with previous reports of plasmid or minichromosome mutation (3).

140 In the 16 clones, overall, 87 different mutations were found on the main chromosome. Of
141 these, 90% consisted of new ISH positions, or of deletions mobilized by existing ISH elements
142 (**Table 3**). Mutation distributions of the minichromosome replicons showed no significant
143 difference in ISH proportion (94 mutations out of 111, on pNRC100; 141 out of 156 on
144 pNRC200). For comparison, we considered a recent *breseq* analysis of 16 *E. coli* genomes
145 following 500 generations evolution with an organic acid (26). Only 18% of the *E. coli*
146 mutations were mediated by insertion sequences. Thus, NRC-1 evolution showed five-fold
147 greater proportion of insertion sequence activity than *E. coli*. Our quantitative analysis of
148 experimentally evolved genomes is consistent with earlier evidence of high ISH activity in
149 halobacterial genomes (38),(47–50),(45).

150 Haloarchaea including *Halobacterium salinarum* species are known for polyploidy (15-
151 25 genome copies per cell) and for ploidy variation among replicons within a cell (51). Our

152 evolved clones showed evidence for variable ploidy between and within replicons. Mean read
153 coverage by replicon was modeled by *breseq* (**Table 4**).

154 Overall, within the ancestor and the evolved clones, the read coverage for the main
155 chromosome was consistent with that of the minichromosome pNRC200. However, the mean
156 coverage of the shorter minichromosome pNRC100 (191 kb) was more than twice that of the
157 main chromosome, for our ancestral NRC-1 and for 12 of the 16 evolved clones. Clones J1, M3-
158 1, K3, S2, and S3 had mean coverage of pNRC100 more than four-fold greater than that of the
159 main chromosome. These high coverage ratios could indicate that our original NRC-1 stock has
160 a double copy number of minichromosome pNRC100, relative to the main chromosome; and that
161 some descendant clones have increased relative copy number. However, the calculations are
162 complicated by wide variation in read coverage between different segments of the same replicon,
163 especially in pNRC100. This variation in read coverage may be caused by internal repeats within
164 the replicon (35). Interpretation of the data is complicated by the presence of massive deletions
165 (Additional File 1, **Table S2**) which comprise up to 50% of the ancestral sequence (for example
166 in clone K1) (50). Variation in read coverage could indicate the presence of plasmid copies with
167 different deletion levels within a given polyploid cell.

168

169 **Acid-evolved clone J3-1 has a growth advantage over a range of pH values.**

170 After 500 generations of serial culture under four conditions, clones were isolated from the
171 evolving populations. The clones were tested for genetic adaptation under various growth
172 conditions. Each evolved clone was cultured in parallel with the ancestral strain NRC-1. The loss
173 of gas vesicles (*Vac*⁻ phenotype) alters their OD₆₀₀ reading (38,47); for this reason, clones that
174 had lost gas vesicles were cultured in parallel with a *Vac*⁻ isolate of NRC-1 ancestor.

175 The growth of acid-evolved J-population clones was compared to that of the NRC-1
176 ancestor (Vac⁺) (**Figs. 1 and 2**). Clone J3-1 reached a significant two-fold higher culture density
177 than did the ancestor when cultured at pH 6.1 or at 6.3 (**Fig. 1B**). Growth advantage was seen for
178 all four replicate cultures of J3-1 at pH 6.1 and at pH 6.3, whereas the difference from NRC-1
179 cultures disappeared at pH 7.2 and at pH 7.5. Thus, strain J3-1 exhibits an acid-specific fitness
180 advantage. The other acid-evolved J-population strains, however, had no significant growth
181 advantage compared to NRC-1, under the conditions tested (**Fig. 2**).

182 **Acid-adapted clones shared mutations in *arcD* and in *arcR*.**

183 We inspected the genomes of acid-adapted populations J and K (acid with iron supplement) for
184 mutations in specific genes that were not found in the populations evolved at pH 7.5. Seven out
185 of eight of the J and K clones (but no M or S clones) had ISH mutations in or upstream of gene
186 VNG_6313G (**Table 2**). This gene was originally classified as encoding a sodium-proton
187 antiporter (*nhaC3*) but was shown instead by physiological experiments to encode an arginine-
188 ornithine antiporter ArcD (52). PCR amplification and Sanger sequencing of the mutant *arcD*
189 alleles confirmed the presence of insertion sequences ISH2 (strains K1 and K4) and ISH4
190 (strains J1, K2-1, K3) (**Table 5**; Additional File 1, **Fig. S2**). Additionally, in J4-2, a partial
191 sequence confirms the presence of 1.1 kb ISH11 insertion flanked by a 10 bp direct repeat, while
192 a large 3000+ bp insertion in K3 returned a partial sequence of ISH4. The partial sequence
193 suggests multiple copies of ISH4, or possibly a composite transposon.

194 Four acid-evolved genomes (J-3, K-1, K2-1, K4-1) and one non-acid-evolved clone (M3-
195 1) possess ISH insertions at different sites in *arcR* on pNRC100 (Additional File 1, **Table S3**).
196 ArcR mediates transcriptional regulation of the *arcABDCR* operon for arginine catabolism
197 (40,41). These components include the arginine deiminase (*arcA*), ornithine

198 carbamoyltransferase (*arcB*), carbamate kinase (*arcC*), and the arginine-ornithine antiporter
199 (*arcD*).

200 For comparison, a remarkably similar system of arginine catabolism reverses acidification
201 for the periodontal bacterium *Streptococcus gordonii* (31,32). Arginine catabolism releases CO₂
202 and two molecules of ammonia, which cause net alkalization. The system mediates tooth biofilm
203 formation by *S. gordonii*. For *E. coli*, the arginine decarboxylase *Adi* reverses acidification at
204 extreme low pH (52). The *adi* system of *E. coli* is induced by acid stress but largely lost by
205 insertion-sequence mutations after long-term evolution in acid (20,22). This suggests a model for
206 acid adaptation in haloarchaea that is remarkably similar to that observed in *E. coli*, in which
207 acid-stress adaptations are knocked down by long-term acid exposure (21).

208

209 **Acid-adapted clones shared mutations in bacteriorhodopsin (*bop*).**

210 In NRC-1, our acid-evolved clones J3-1 and K1 each contained an ISH element in the gene *bop*
211 that encodes the light-driven proton pump bacteriorhodopsin (35). The J3-1 allele was confirmed
212 by Sanger sequence as a 1.1 kb insertion of ISH1 with an eight bp target site duplication in *bop*
213 (**Table 5**; Additional File 1, **Fig. S2**). This exact mutation has been previously studied in
214 bacteriorhodopsin mutants, and was in fact the first transposable element identified in
215 haloarchaea (35). This particular target site duplication was shared with acid-evolved clone K1.
216 At a different position, a *bop* ISH insertion was found in one of the M population clones (M3-1)
217 which had not undergone acid selection, consistent with previous spontaneous insertions in this
218 gene.

219 The *bop* and *arcD* mutations were found together in J3-1, but also in acid-adapted K1,
220 which did not show a significant phenotype under our conditions tested. We inspected strain J3-1

221 for candidate mutations that might be responsible for this strain's unique degree of adaptation at
222 low pH. Overall, the J3-1 genome had 16 mutations compared to the NRC-1 ancestor (**Table 6**).
223 Of these, only one mutation affected a gene not affected in any other evolved clone. This is a
224 missense mutation in a ferredoxin gene (*VNG1561*) resulting in a conservative change from
225 lysine to arginine. Mutations were also found affecting several proteins involved in
226 transcriptional regulation, which in combination might contribute to the acid fitness phenotype.

227 **Clones evolved at pH 7.5 show no increase in relative fitness.** All evolved clones from
228 generation 500 with Vac⁻ phenotypes were grown over 200 hours in unbuffered CM⁺ medium
229 without acid or iron amendment and compared to the growth phenotype of the NRC-1 Vac⁻
230 control strain (**Fig. S2A**). Similarly, the growth phenotypes in unstressed medium of Vac⁺ clones
231 from the 500-generation populations that retained them were compared to that of the NRC-1
232 Vac⁺ ancestor (**Fig. S2B**). None of the M populations show a significant growth advantage
233 compared to the ancestral strain (Additional File 1, **Fig. S3A and B**).

234 Growth curves were also conducted for clones from the S populations (evolved with 600
235 μM FeSO₄). Media contained CM⁺ pH 7.5 with 100 mM MOPS and 600 μM FeSO₄. All
236 evolved clones were persistent Vac⁻ mutants at generation 500 and were therefore compared to
237 an NRC-1 Vac⁻ control (Additional File 1, **Fig. S4**). No significant differences were observed.

238 **Multiple clones lost gas vesicles and arsenic resistance.** Under laboratory conditions,
239 gas vesicle-producing (Vac⁺) NRC-1 clones have high rates of spontaneous mutation to a
240 vesicle-deficient (Vac⁻) phenotype due to mutations in *gvp* on pNRC100 (38,47). Twelve out of
241 sixteen of our evolved clones, including representatives of each selection type, had lost genes
242 required for gas vesicle nanoparticle production (*gvp*) (53–55). Cultures were oxygenated
243 continually by rotating in a bath, effectively eliminating the competitive advantage of producing

244 gas vesicles in oxygen-limiting environments. Thus, as expected, many insertions and deletions
245 were found that had eliminated gas vesicles (45,47). We characterized gas vesicle phenotypes
246 every 100 generations for the stressed condition populations. These Vac phenotypes (loss of gas
247 vesicle nanoparticles) are presented by population and organized by respective evolution
248 condition in **Table 7**. All evolving populations showed loss of gas vesicle production in some
249 cells. By generation 500, the Vac⁻ phenotype was prevalent in all populations. There was no
250 significant correlation with pH or with iron amendment.

251 In addition, 13/16 evolved clones had lost the major arsenic resistance operon (*ars*)
252 encoded on pNRC100 (7). Other mutations affecting transcriptional regulators and initiation
253 factors occurred in parallel across multiple populations. These and other parallel mutations are
254 summarized in **Table 2**. Various hot spots for mutation appear, many of which are caused by
255 ISH insertions or ISH-mediated deletions.

256

257 DISCUSSION

258 Here we report one of the first evolution experiments to be conducted on a haloarchaeon. A
259 previous evolution experiment involves selection of mutants resistant to ionizing radiation (28).

260 We compared four environmental conditions: low pH versus optimal pH 7.5, with or
261 without iron supplementation. Overall, in the 500-generation evolved strains, we found a striking
262 pattern of large ISH-mediated deletions, particularly in the two minichromosomes (Additional
263 File 1, **Tables S1-S3**). For comparison, in *E. coli*, experimental evolution for 2,000 generations
264 at low pH yields only occasional large deletions (20,21). However, after just 500 generations of
265 evolution in the haloarchaeon NRC-1, every evolved clone contained several large-scale
266 deletions. ISH insertion mutations greatly outnumbered SNPs. These types of changes reflect
267 frequent DNA rearrangements and genetic variability observed previously in NRC-1 (35,39,49).

268 The acid-adapted NRC-1 populations showed a striking prevalence of mutations affecting
269 the *arcD* and *arcR* components of arginine transport and catabolism. Arginine catabolism with
270 ammonia release plays a major role in reversing acidity for Gram-positive and Gram-negative
271 bacteria. It is striking to see how the role of acid-dependent arginine catabolism may extend to
272 haloarchaea. The arginase/arginine deiminase family (COG0010) represents a set of orthologs
273 proposed to be among those transferred horizontally to archaea from an ancient bacterial
274 ancestor (56).

275 The ISH insertions seen in acid-adapted clones would be expected to knock out the
276 arginine system, as seen in *E. coli* experimental evolution with acid (20,41). The reason for the
277 evolutionary loss is proposed to be a readjustment to long-term acid exposure, for which the
278 sustained induction of arginine catabolism becomes counterproductive. It is interesting to find
279 evidence for a similar evolutionary mechanism in a haloarchaeon.

280 In addition, the acid-evolved strains J3-1 and K1 show an identical insertion mutation
281 affecting the bacteriorhodopsin *bop* gene. The loss of *bop* may be neutral or advantageous under
282 low external pH, where a high proton motive force already exists. The bacteriorhodopsin pump
283 could be a source of proton leakage at high PMF.

284 The acid-fitness advantage of clone J3-1 could arise from a single mutation unique to J3-
285 1, such as the missense mutation in a ferredoxin that is unique to J3-1. More likely, however,
286 acid fitness arises from a cumulative effect of loss of function mutations in a number of other
287 genes including *arcA*, *arcR*, and *bop*. It is possible that some unknown factor accounts for the
288 acid-fitness phenotype exhibited by J3-1 under the conditions tested. Nonetheless, it is
289 interesting that the three genes with mutations prevalent in acid-evolved strains all encode
290 products involved in proton consumption or export.

291 Our findings support previous reports of the importance of ISH elements in haloarchaeal
292 evolution (45), and the observations in *Sulfolobus* that large deletions and loss of function
293 mutations are fitness tradeoffs for surviving in stressful environments (57). Large deletions and
294 IS insertions are also common in experimental evolution of bacteria (20,21,27,58). We also find
295 evidence for accumulation of ploidy changes for the shorter minichromosome, pNRC100 (51).
296 We show that experimental evolution is an effective approach to identify candidate genes for
297 environmental stress response in a haloarchaeon.

298

299 MATERIALS AND METHODS

300

301 ***Halobacterium* strains and media.** All evolved clones were derived from a stock of302 *Halobacterium* sp. NRC-1 from the laboratory of Shiladitya DasSarma (3). Liquid cultures were303 grown in Complex Medium Plus Trace Metals (CM⁺) based on Ref (2), Protocol 25: 250 g/l304 NaCl, 20 g/l MgSO₄•7H₂O, 2 g/l KCl, 3 g/l Na₃C₆H₅O₇•2H₂O, 10 g/l Oxoid Peptone, and 100305 μl/l Trace Metals (3.5 g/l FeSO₄•7H₂O, 0.88 g/l ZnSO₄•7H₂O, 0.66 g/l MnSO₄•H₂O, and 0.2 g/l306 CuSO₄•5H₂O dissolved 0.1M HCl) with supplements as needed for the conditions examined307 (59). CM⁺ solid medium included addition of 20 g/l granulated agar. All cultures were incubated

308 at 42°C with rotation. Cultures on solid media were incubated at 42°C for 7–10 days until

309 colonies reached approximately 1 mm in diameter. A Vac⁻ mutant of our NRC-1 stock culture310 was obtained by picking a Vac⁻ colony followed by three restreaks on CM⁺ agar.311 Liquid CM⁺ media for experimental evolution was made with either 100mM PIPES

312 (pKa=6.8) or 100mM MOPS (pKa=7.2) buffer with pH adjusted using 5 M NaOH or 5 M HCl as

313 needed, followed by filter sterilization. 100 mM FeSO₄ stock was prepared in deionized water

314 and filter-sterilized before every other dilution during serial batch culture evolution. Sterilized

315 FeSO₄ stock was added to buffered CM⁺ after filter sterilization. For freezer stocks, live cultures

316 were mixed 1:1 with a 50% glycerol, 50% complex medium basal salts mixture as a

317 cryoprotectant. Complex medium basal salts were 250 g/l NaCl, 20 g/l MgSO₄•7H₂O, 2 g/l KCl,318 3 g/l Na₃C₆H₅O₇•2H₂O. Acidic, control, iron-rich and acidic, and iron-rich media used in the319 evolution consisted of: CM⁺ pH 6.5 with 100 mM PIPES (populations J1-J4), CM⁺ pH 7.5 with320 100 mM MOPS (populations M1-M4), CM⁺ pH 6.5 (or pH 6.3) with 100 mM PIPES 600 μM321 FeSO₄ (populations K1-K4), and CM⁺ pH 7.5 with 100 mM MOPS 600 μM FeSO₄ (populations

322 S1-S4).

323 **Experimental evolution.** A total of 16 populations (four per evolution condition) were
324 founded from a 5 ml CM⁺ tube culture (7-10 days incubation) of *Halobacterium* sp. NRC-1 that
325 was diluted 500-fold and incubated 4 days in a 42°C shaker bath at 200 rpm. At the end of the
326 fourth day, 10 µl of the previous culture was diluted into 5 ml of fresh CM⁺ media amended as
327 necessary for the respective stress condition. The resulting 1:500 dilutions yield approximately
328 nine generations per dilution cycle. If cultures did not reach a healthy cell density as qualitatively
329 evaluated for each dilution, 1:100 or 1:250 dilutions were performed to prevent loss of evolving
330 populations. Alternative dilution concentrations were factored into total generation counts at the
331 end of experimental evolution. When evolution was interrupted, the populations were revived by
332 1:250 dilutions from freezer stocks of the previous dilution. Freezer stocks comprised 1 ml
333 liquid, mature haloarchaea culture for each evolving population and 0.5 ml glycerol/basal salts
334 mixture, stored in 2 ml Wheaton brand vials and frozen at -80°C for each dilution, totaling 16
335 freezer stocks every four days. A summary of the evolution procedure is presented in **Figure S1**.

336 **Clone selection.** Clones were isolated by plating 10 µl of culture from generation 100,
337 200, 300, 400, and 500 from freezer stocks for all 16 evolving populations on CM⁺ agar plates,
338 followed by incubation in a sealed container at 42°C for 7–10 days. Isolated colonies were then
339 selected for diverse Vac phenotypes, streaked on fresh CM⁺ agar plates, and incubated a second
340 time. The process was repeated a third time to ensure isolation of select genetically pure clones.
341 Colonies from the third streak were grown in unbuffered CM⁺ pH 7.2, and stocks were frozen for
342 later phenotype and genotype characterization. One clone was isolated from each population
343 every 100 generations. For populations that presented mixed gas vesicle production phenotypes,
344 we isolated both a Vac⁺ clone and a Vac⁻ clone. In total, 75 clones were isolated from generation
345 100, 200, 300, and 400 of the evolution. Clones were similarly isolated from generation 500;

346 however, the first streak was taken directly from evolving populations, rather than from frozen
347 stock in Wheaton vials. Two clones were isolated from each population at 500 generations, for a
348 total of 32 clones.

349 **Gas vesicle formation phenotype analysis.** Vesicle formation phenotype was assessed
350 qualitatively based on the relative translucence of plated colonies and denoted as Vac⁺ or Vac⁻ as
351 appropriate (2,47). If more than one Vac phenotype was observed in a streak during strain
352 isolation, the phenotypic variant colonies were re-streaked and treated as separate clonal isolates.
353 Vac phenotypes were evaluated for persistence with each streak based on whether or not Vac⁺
354 colonies yielded >1% Vac⁻ progeny or vice versa.

355 **Growth assays.** The generation 500 clones used in these assays are summarized in **Table**
356 **1.** Clones were cultured in unbuffered CM⁺ at pH 7.2, and incubated for four days in a 42°C
357 shaker bath with 200 rpm orbital aeration. Over-week starter cultures were diluted 1:1000 into
358 new test tubes with 5 ml of the appropriate test condition media. A media blank was included for
359 each media condition, and each clone was tested with four to eight biological replicates,
360 depending on the assay. Immediately after inoculation, OD₆₀₀ values were recorded by a
361 Spectramax 384+ spectrophotometer at 600 nm using Softmax Pro version 6.4.2. Daily readings
362 were taken for nine days. Media for these tests included CM⁺ pH 6.3 100 mM PIPES and CM⁺
363 pH 6.1 100 mM PIPES for J clones. M clones were tested in CM⁺ pH 7.5 100 mM MOPS. K
364 clones were tested in CM⁺ pH 6.3 100 mM PIPES 600 μM FeSO₄ and CM⁺ pH 6.1 100 mM
365 PIPES 600 μM FeSO₄. S clones were tested in CM⁺ pH 7.5 100 mM MOPS 600 μM FeSO₄.

366 To test for pH-dependent growth advantages, evolved clones that showed growth
367 advantages over ancestor in their respective evolution stress conditions under which they were
368 evolved were also tested for growth advantages in pH conditions other than those in which they

369 evolved. For these experiments, J3-1 was cultured in CM+ pH 7.5 100 mM MOPS and compared
370 using a Vac⁺ NRC-1 control, M3-1 was cultured in CM+ pH 6.1 100 mM PIPES and compared
371 using a Vac⁺ NRC-1 control, and K2-1 was cultured in CM+ pH 7.5 100 mM MOPS 600 μ M
372 FeSO₄ and compared to both Vac⁺ and Vac⁻ NRC-1 controls due to gas vesicle phenotype
373 ambiguity. Analysis was carried out with comparisons to an ancestral control expressing the
374 same Vac phenotype as the evolved clone.

375 All growth assays were evaluated for statistical significance using ANOVA test with
376 Tukey post-hoc or paired T-test using base R and agricolae package. Comparisons between
377 clones were made using post log-phase endpoint “E” values for optical density at six days post
378 inoculation.

379 **DNA extraction and genome sequencing.** Genomic DNA was isolated from the 16
380 evolved clones and the ancestor NRC-1 using an Epicentre MasterPure Gram Positive DNA
381 Extraction Kit and a modified procedure. Lysozyme was omitted, and DNA purity and
382 concentration was determined using a Thermo Scientific NanoDrop 2000. Genomic DNA was
383 sequenced at the Michigan State University Research Technology Support Facility (RTSF)
384 Genomics Core. Libraries were prepared using the Illumina TruSeq Nano DNA library
385 preparation kit for Illumina MiSeq sequencing and loaded on a MiSeq flow cell after library
386 validation and quantitation. Sequencing was completed using a 2- by 250-bp paired-end format
387 using Illumina 500 cycle V2 reagent cartridge. Illumina Real Time Analysis (RTA) v1.18.54
388 performed base calling, and the output of the RTA was demultiplexed and converted to FastQ
389 format with Illumina Bcl2fastq v1.8.4.

390 **Sequence assembly and analysis using the *breseq* computational pipeline.** The
391 computational pipeline *breseq* version 0.27.1 was used to assemble and annotate the resulting

392 Illumina reads of the evolved clones (42–44). The current *breseq* version is optimized to detect
393 IS element insertions and IS-mediated deletions, as well as SNPs and other mutations in *E. coli*
394 (19). Illumina reads were mapped to the *Halobacterium* sp. NRC-1 reference genome (NCBI
395 GenBank assembly accession GCA_000006805.1). Mutations were predicted by *breseq* through
396 sequence comparisons between the evolved and ancestral clones.

397 The Integrative Genomics Viewer (IGV) from the Broad Institute at Massachusetts
398 Institute of Technology was used to visualize the assembly and mutations in the evolved clonal
399 sequences mapped to the reference NRC-1 genome (60). Each replicon was mapped separately
400 using the following RefSeq IDs: NC_002607.1 (main chromosome), NC_001869.1 (pNRC100),
401 and NC_002608.1 (pNRC200). Sequence mean coverage in each evolved clone was estimated
402 using the *breseq* fit dispersion function.

403 **PCR confirmation of ISH insertions.** PCR primers (Table 5) were designed to confirm
404 the presence of insertion sequences at hypothetical target site duplications. Primers adhered to
405 the following specifications using Sigma Aldrich Oligo Evaluator: 19-22 bp in length, GC
406 content between 40-60%, no single bp runs >3, weak to no secondary structure, and no primer
407 dimer. Oligos were checked for sequence identity of ≤ 13 bp to any part of the NRC-1 genome
408 other than the target site using NCBI BLAST. We ran 50- μ l PCR using Applied Biosystems
409 Amplitaq Gold 360 Master Mix according to the package insert with 50 μ l reaction containing
410 GC enhancer. To assess insert length, 10 μ l of PCR product was electrophoresed in a 1% agarose
411 gel. PCR products were then purified either by Qiagen QIAquick PCR Purification Kit or
412 QIAquick Gel Extraction Kit.

413 **Accession number for sequenced genomes.** Sequenced genomes are deposited under
414 SRA accession number SRP195828.

415

416 ACKNOWLEDGEMENTS

417 This project was supported by the National Science Foundation award MCB-1613278 to

418 Joan Slonczewski; by the 2016 NASA Astrobiology Program Early Career Collaboration Award

419 to Karina Kunka and Jessie Griffith; and by NASA Exobiology grants NNX15AM07G and

420 NNH18ZDA001N to Shiladitya DasSarma. We thank Friedhelm Pfeiffer for pointing out the

421 *arcD* annotation. We thank Landon Porter for expert technical assistance.

422

423 TABLES AND FIGURES

424

425 **Table 1. Strains used in this study**

Strain Name	Description	Generation	Evolution Condition	Vac +/- *	Source
NRC-1	Ancestor strain	0	--	+	S. DasSarma
NRC-1	Ancestor strain	0	--	-	S. DasSarma
JLSHA075	Clone J1	500	pH 6.3 100 mM PIPES	-	This study
JLSHA078	Clone J2-2	500		-	This study
JLSHA079	Clone J3-1	500		+	This study
JLSHA082	Clone J4-2	500		-	This study
JLSHA083	Clone M1	500	pH 7.5 100 mM MOPS	-	This study
JLSHA086	Clone M2-2	500		-	This study
JLSHA087	Clone M3-1	500		+	This study
JLSHA089	Clone M4-1	500		+	This study
JLSHA091	Clone K1	500	pH 6.3 100 mM PIPES 600 μ M Fe ²⁺	-	This study
JLSHA093	Clone K2-1	500		+	This study
JLSHA095	Clone K3	500		-	This study
JLSHA097	Clone K4	500		-	This study
JLSHA099	Clone S1	500	pH 7.5 100 mM MOPS 600 μ M Fe ²⁺	-	This study
JLSHA101	Clone S2	500		-	This study
JLSHA103	Clone S3	500		-	This study
JLSHA105	Clone S4	500		-	This study

426 *"+" indicates gas vesicle-forming, "--" indicates non gas vesicle-forming

Table 2. Selected mutations found in evolved clones.*†

Replicon	Start bp	pH 6.3				pH 7.5				pH 6.3, Fe				pH 7.5, Fe				Annotation	Gene Description
		J1	J2-2	J3-1	J4-2	M1	M2-2	M3-1	M4-1	K1	K2-1	K3	K4	S1	S2	S3	S4		
Chromosome	~15,266																	ISH: intergenic	(vng0018H→) / (vng0019H→)
Chromosome	~23,074																	ISH: intergenic	(vng0027H←) / (→vng0028C)
Chromosome	~25,216																	ISH: intergenic	(vng0029H←) / (→vng0030H)
Chromosome	~29,154																	ISH: coding	[vng0032H→]
Chromosome	~48,587																	ISH8-3 mediated	(vng0053H→) / [→vng0053H]
Chromosome	~52,664																	ISH: intergenic	(vng0056H←) / (→vng0057 O_antigen polymerase)
Chromosome	~181,512																	ISH: coding	[vng0215C←]
Chromosome	414,229																	A675A (GCG→GCT)	[vng0053H7←] (TRAP transporter permease)
Chromosome	~749,543																	ISH: coding	[vng0985H→]
Chromosome	~753,552																	ISH: intergenic and (T)9→8	(vng0986H→) / (→vng0987H)
Chromosome	~754,476																	ISH: coding	[vng0989C←] xcd (integrase)
Chromosome	~772,459																	ISH: intergenic	(vng1007H←) / (→vng1008G) flaA1a (flagellin A1 precursor)
Chromosome	~1,089,129																	ISH: coding	[vng1467G→] bop (rhodopsin).
Chromosome	~1,229,749																	ISH: coding/ ISH2 deletion	[vng1650H←]
PNRC100	0																	ISH7-1 deleted	[vng7001←] - [←vng_RS13745]
PNRC100	~9,546																	ISH3-1	[vng_RS13755→] / (→vng_RS12260)
PNRC100	~14,052																	ISH3-1	(vng_RS12260←) / (→vng7012)
PNRC100	~15,600																	ISH8-3, 8-1	(vng7012→) - (←vng_RS12360) Gas vesicle protein cluster (deleted)
PNRC100	~41,820																	ISH5-1*, 8-5	(vng7039→) - (→vng_RS13770) yobE, XRE regulator, MFS transporter, thioredoxin, deoxyribonuclease, cell division control protein (all deleted)
PNRC100	~71,208																	ISH2	(vng_RS13790→) - [←vng7073] SOS response peptidase (deleted)
PNRC100	~75,169																	ISH2	(vng7074←) - (←vng7078)
PNRC100	~81,100																	ISH8-3, 3-1	[vng_RS12615←] - [→vng7079]
PNRC100	~83,375																	ISH3-1, 7-2	(vng7080←) - [←vng7085]
PNRC100	~87,224																	V→L (GTG→CTG)	[vng7085←]
PNRC100	~133,744																	ISH8-2, 3-3	(vng_RS12830←) - (→vng7127) Arsenic resistance operon (deleted)
PNRC100	~143,907																	ISH3-3, 2	(vng_RS12880→) - [→vng7136] ssDNA-binding protein A (deleted)
PNRC100	~150,769																	ISH2, 3-2	(vng7136←) / (←vng_RS12925)
PNRC100	~152,257																	ISH2, 3-2	[vng_RS13845←]
PNRC100	~153,526																	ISH3-2, 2	[←vng_RS13850]
PNRC100	~164,889																	ISH8-5, 5-1	(vng_RS13865←) - (←vng7170) Thioredoxin reductase, boa3 (bacteriorhodopsin activator), phoT1 phosphate transporter, cydBA cytochrome d oxidase (all deleted).

Replicon	Start bp	J1	J2-2	J3-1	J4-2	M1	M2-2	M3-1	M4-1	K1	K2-1	K3	K4	S1	S2	S3	S4	Annotation	Gene Description
PNRC200	0																	ISH 7-1 deleted	(vng6001H←) - [←vng6011H]
PNRC200	~7,477																	ISH: coding	[vng6011H←]
PNRC200	~9,569																	ISH 3-1	[vng6013G→] / (←vng_RS10565)
PNRC200	~14052																	ISH 3-1	(vng_RS10565←) / (→vng6016H)
PNRC200	~15,594																	ISH 8-3, 8-1	(vng6016H→) - (→vng_RS10665)
PNRC200	~41,819																	ISH 5-1*, 8-5	(vng6053G→) - (→vng6079H) Thioredoxin reductase, boa3 (bacteriorhodopsin activator), phoT1 phosphate transporter), cydBA cytochrome d oxidase (all deleted).
PNRC200	~71,208																	ISH 2	(vng6094H→) - [←vng6097C] SOS response peptidase (deleted)
PNRC200	~75,168																	ISH 2, 8-4	(vng6099H←) - (←vng6105H)
PNRC200	~81,101																	ISH 8-4, 3-1	[vng_RS10920←] / [→vng_RS10925]
PNRC200	~83,374																	ISH 3-1, 7-2	(vng6112H←) - [←vng6119H]
PNRC200	~87,224																	V→L(GTG→CTG)	[vng6119H←]
PNRC200	~138,366																	ISH 8-4	[vng6162H←] - [→vng6181H] orc2 (cell division control protein 6), nbp2 (nucleic acid binding protein), srl1 (ATPase), trkA2 (TRK K+ uptake system protein), kdpABC (K+ ATPase), cat3 (cationic amino acid transporter) (all deleted).
PNRC200	~140,521																	ISH: coding	[vng6164G←] orc2 (orc/cell division control protein 6).
PNRC200	~244,149																	ISH: coding	[vng6313G←] arcD Arginine:ornithine antiporter (formerly annotated nhaC3)
PNRC200	~248,490																	ISH: coding	[vng6318G←] arcR (Arginine catabolism transcriptional regulator)
PNRC200	~262,599																	ISH 3-2, 8-3 / ISH 8-3 deleted	(vng_RS11685←) / (→vng6331H)
PNRC200	~272,000																	ISH 6, 3-2	(vng6341H→) / (←vng_RS13610)
PNRC200	~274,345																	ISH 3-2, 8-4	(vng_RS11735←) / (←vng6345H)
PNRC200	~278,031																	ISH 8-4, 2	[vng6346H←] - (←vng6393H) DNA polymerase I, cdc6 cell division control protein, HNH endonuclease, MarR family transcriptional regulator, AbrB family transcriptional regulator, L-lactate permease (all deleted)
PNRC200	~278,118																	ISH: coding	[vng6346H←]
PNRC200	~279,927																	ISH: intergenic	(vng6348H←) / (←vng6349C)
PNRC200	~293,402																	ISH: coding	[vng6364H←]
PNRC200	~309,253																	ISH 2, 8-3	(vng6393H←) - (←vng6395H)
PNRC200	~311,206																	ISH 8-3, 11	(vng6396H→) - (←vng6420H) arsR transcriptional regulator, phzF phenazine biosynthesis
PNRC200	~324,384																	ISH 11	(vng_RS12000→) - (→vng6441H)

* “Annotation” column code: “ISH *** mediated” = flanking ISH elements, if relevant. Mutation codes: blue = missense, green = silent.

“Gene” column code: (mutation starts or ends before this gene name), → ← indicates gene directionality, [mutation starts, ends, or is entirely contained within this gene name], “-” indicates intervening omitted genes found in description, “/” indicates mutation is between two genes.

Highlight indicates mutations associated with acid evolution.

†This chart does not indicate shared lineage through identical mutations. For a complete list of mutations, see **Tables S1-S3**.

Table 3. Classes of mutations found in evolved clones.*

Chromosome																	
Mutation Type	Low pH				Control				Low pH and Iron-rich				Iron-rich				Mutation Sum
	J1	J2-1	J3-1	J4-2	M1	M2-2	M3-1	M4-1	K1	K2-1	K3	K4	S1	S2	S3	S4	
TSD	4	5	3	5	1	4	4	1	7	6	5	5	1	6	6	1	64
Deletion	1	1	0	1	1	1	2	2	1	1	0	1	0	0	1	0	13
SNP	0	0	1	0	1	2	1	1	1	1	0	1	0	0	0	1	10
Insertion	0	0	0	0	0	0	0	0	0	0	0	0	0	0	0	0	0
Chromosome Total	5	6	4	6	3	7	7	4	9	8	5	7	1	6	7	2	87

PNRC100																	
Mutation Type	J1	J2-1	J3-1	J4-2	M1	M2-2	M3-1	M4-1	K1	K2-1	K3	K4	S1	S2	S3	S4	Mutation Sum
	TSD	0	1	0	0	0	7	0	0	3	0	0	0	2	2	0	
Deletion	5	3	4	7	2	0	6	3	17	8	8	10	4	3	5	4	89
SNP	2	0	0	0	0	6	0	0	0	0	3	5	0	0	0	0	16
Insertion	0	0	0	0	0	0	0	0	0	0	0	0	0	0	0	0	0
PNRC100 Total	7	4	4	7	2	13	6	3	20	8	11	15	6	5	5	4	120

PNRC200																	
Mutation Type	J1	J2-1	J3-1	J4-2	M1	M2-2	M3-1	M4-1	K1	K2-1	K3	K4	S1	S2	S3	S4	Mutation Sum
	TSD	1	1	2	1	1	4	0	0	3	7	3	7	2	0	3	
Deletion	6	4	6	7	8	14	15	7	15	5	4	5	3	5	6	5	115
SNP	1	0	0	0	0	5	0	0	1	0	3	5	0	0	0	0	15
Insertion	1	0	0	0	0	0	0	0	0	0	0	0	0	0	0	0	1
PNRC200 Total	9	5	8	8	9	23	15	7	19	12	10	17	5	5	9	10	171

Complete genome																	
Mutation Type	J1	J2-1	J3-1	J4-2	M1	M2-2	M3-1	M4-1	K1	K2-1	K3	K4	S1	S2	S3	S4	Mutation Sum
	TSD	5	7	5	6	2	15	4	1	13	13	8	12	5	8	9	
Deletion	12	8	10	15	11	15	23	12	33	14	12	16	7	8	12	9	217
SNP	3	0	1	0	1	13	1	1	2	1	6	11	0	0	0	1	41
Insertion	1	0	0	0	0	0	0	0	0	0	0	0	0	0	0	0	1
Complete Total	21	15	16	21	14	43	28	14	48	28	26	39	12	16	21	16	378

*TSD = target site duplication indicating ISH; SNP = single nucleotide polymorphism.

Table 4. Coverage depth for NRC-1 and evolved clones.

Strain	Main chromosome		pNRC100		pNRC200	
	Read depth*	SD	Read depth*	SD	Read depth*	SD
NRC-1	50	10	128	15	64	10
J1	46	9	338	29	53	9
J2-2	41	9	156	14	48	8
J3-1	57	11	87	13	91	14
J4-2	64	11	137	15	85	13
M1	49	9	187	18	44	7
M2-2	67	11	165	17	62	10
M3-1	49	10	275	26	54	9
M4-1	65	11	162	13	75	11
K1	74	13	72	10	63	11
K2-1	72	13	NA	NA	76	11
K3	52	10	363	29	92	13
K4	59	11	96	11	71	15
S1	39	8	125	15	44	8
S2	42	9	169	18	34	7
S3	47	10	202	16	55	9
S4	46	9	185	14	37	7

*Mean copy number of sequence across the replicon, according to the *breseq* fitted dispersion model. SD = standard deviation predicted by the model.

Table 5. ISH insertions confirmed by PCR in acid-adapted strains.

Strain	Gene Mutation	ISH	Primer 1	Primer 2
J1	<i>arcD</i> insertion	ISH4	GATAACGATGGACATGTACT	GTCGGTATCGTTCTTTTGGG
J3-1	<i>arcR</i> insertion	ISH8-2	ACTGGTGTGGAGTTTCCGTG	ATCTCACGATCAAGGACGGTGTT
J3-1	<i>bop</i> insertion	ISH1	GAGTTACACACATATCCTCG	GCGTAGAATTTCTTTGCATC
J4-2	<i>arcD</i> insertion	ISH11	GATAACGATGGACATGTACT	GTCGGTATCGTTCTTTTGGG
K1	<i>arcD</i> insertion	ISH2	GATAACGATGGACATGTACT	GTCGGTATCGTTCTTTTGGG
K1	<i>arcR</i>	ISH8-2	ACTGGTGTGGAGTTTCCGTG	ATCTCACGATCAAGGACGGTGTT
K2-1	<i>arcD</i> insertion	ISH4	GATAACGATGGACATGTACT	GTCGGTATCGTTCTTTTGGG
K3	<i>arcD</i> insertion	ISH4	GATAACGATGGACATGTACT	GTCGGTATCGTTCTTTTGGG
K4	<i>arcD</i> insertion	ISH2	GATAACGATGGACATGTACT	GTCGGTATCGTTCTTTTGGG
K4	<i>arcR</i>	ISH3-2	AGAAGTCGTTTCAGAAACAGG	GATACGCGATCAACGACGA

Table 6. Acid-evolved clone J3-1 mutations.* †

Replicon	Start bp	End bp	Mutation	Annotation	Description
Chromosome	749,943	749,954	(11 bp) 1→2	ISH: coding (562/2007 nt)	[vng0985H→]
Chromosome	1,089,129	1,089,137	(8 bp) 1→2	ISH: coding (15/789 nt)	[vng1467G→] bop (rhodopsin).
Chromosome	1,163,363		A→G	K197R (AAA→AGA)	[vng1561→] Ferredoxin
Chromosome	1,229,749	1,229,760	(11 bp) 1→2	ISH: coding (582/849 nt)	In vng1650.
PNRC100	0	7,788	Δ7788 bp	ISH7-1 deleted	[vng7001←] - [←vng_RS13745]
PNRC100	71,210	74,656	Δ3447 bp	ISH2 mediated	(vng_RS13790→) - [←vng7073] SOS response peptidase (deleted)
PNRC100	133,743	142,521	Δ8779 bp	ISH8-2, 3-3 mediated	(vng_RS12830←) - (→vng7127) Arsenic resistance operon (deleted)
PNRC100	143,909	150,253	Δ6345 bp	ISH3-3, 2 mediated	(vng_RS12880→) - [→vng7136] ssDNA-binding protein A (deleted)
PNRC200	0	7,760	Δ7760 bp	ISH 7-1 deleted	(vng6001H←) - [←vng6011H]
PNRC200	71,219	74,595	Δ3377 bp	ISH 2 mediated	(vng6094H→) - [←vng6097C] SOS response peptidase (deleted)
PNRC200	244,422	244,430	9 bp (1→2)	ISH: intergenic	(vng6313G←) / (vng6315G←) arcD Arginine:ornithine antiporter / ornithine carbamoyltransferase
PNRC200	249,147	249,157	11 bp (1→2)	ISH: coding	[vng6318G←] arcR Arginine catabolism transcriptional regulator
PNRC200	262,603	265,437	Δ2835 bp	ISH 3-2, 8-3 mediated/ ISH 8-3 deleted	(vng_RS11685←) / (→vng6331H)
PNRC200	309,256	309,812	Δ557 bp	ISH 2, 8-3 mediated	(vng6393H←) - (←vng6395H)
PNRC200	311,213	323,320	Δ12108 bp	ISH 8-3, 11 mediated	(vng6396H→) - (←vng6420H) arsR transcriptional regulator, phzF phenazine biosynthesis
PNRC200	324,386	332,792	Δ8407 bp	ISH 11 mediated	(vng_RS12000→) - (→vng6441H)

* “Annotation” column code: “ISH *** mediated” = flanking ISH elements, [missense mutations in blue](#).

“Gene” column code: (mutation starts or ends before this gene name), → ← indicates gene directionality, [mutation starts, ends, or is entirely contained within this gene name], “-” indicates intervening omitted genes found in description, “/” indicates mutation is between two genes.

† Highlight indicates mutations associated with acid evolution.

Table 7: Change in gas vesicle phenotype during evolution across populations*

Media condition	Strain	Generation				
		100	200	300	400	500
pH 6.3 100 mM PIPES	J1	+	Vac ^{+/-}	-	-	-
	J2	+	Vac ^{+/-}	-	-	Vac ^{+/-}
	J3	>1% Vac ⁻	Vac ^{+/-}	-	-	Vac ^{+/-}
	J4	+	+	-	-	Vac ^{+/-}
pH 7.5 100 mM MOPS	M1	+	+	+	Vac ^{+/-}	Vac ^{+/-}
	M2	+	+	+	Vac ^{+/-}	Vac ^{+/-}
	M3	+	+	+	Vac ^{+/-}	Vac ^{+/-}
	M4	+	>1% Vac ⁻	+	+	Vac ^{+/-}
pH 6.3 100 mM PIPES 600 μ M FeSO ₄	K1	+	Vac ^{+/-}	-	Vac ^{+/-}	Vac ^{+/-}
	K2	Vac ^{+/-}	Vac ^{+/-}	-	-	Vac ^{+/-}
	K3	+	Vac ^{+/-}	-	-	Vac ^{+/-}
	K4	+	Vac ^{+/-}	-	-	Vac ^{+/-}
pH 7.5 100 mM MOPS 600 μ M FeSO ₄	S1	+	+	-	-	-
	S2	+	+	-	-	-
	S3	+	+	-	-	-
	S4	+	+	+	-	-

* “+” indicates gas vesicle-forming, “-” indicates non gas vesicle-forming

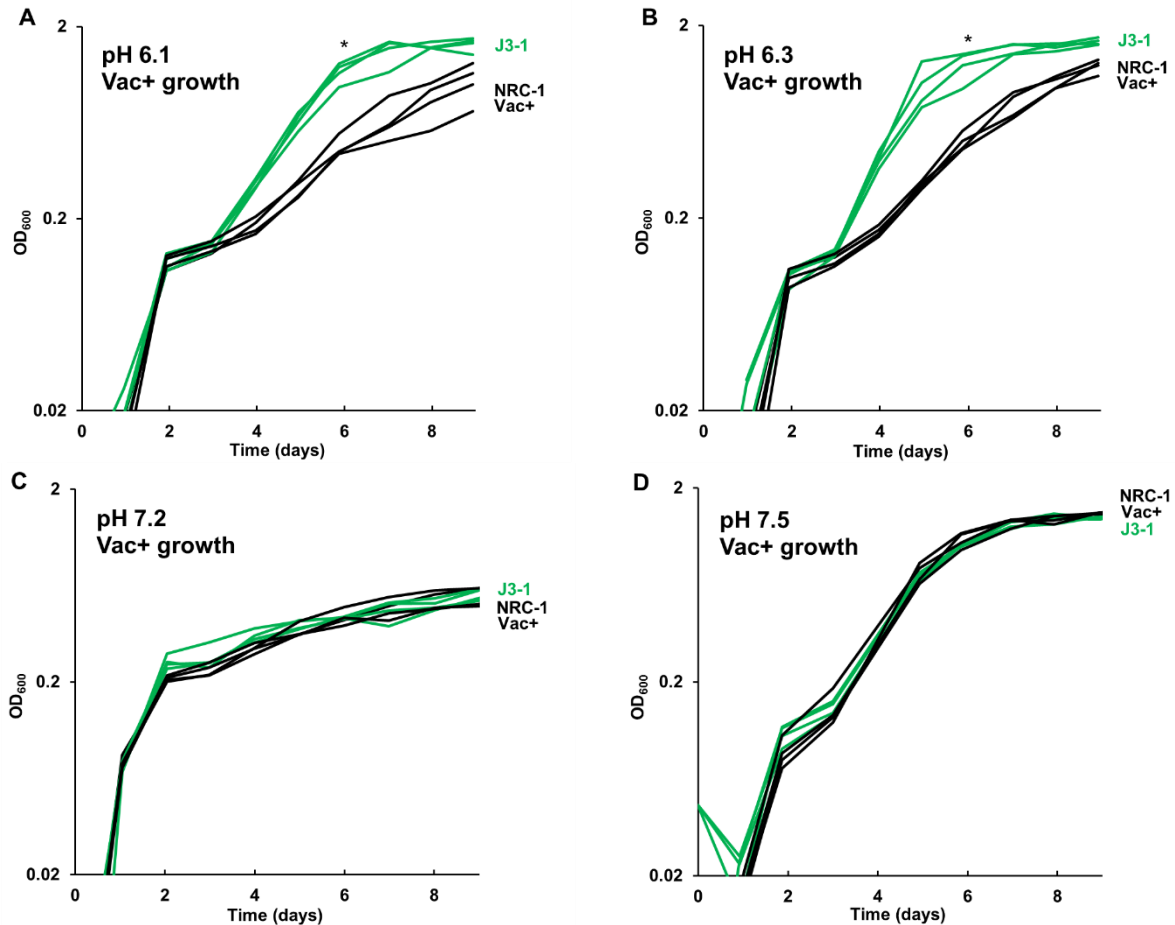


Figure 1. Acid-evolved clone J3-1 shows a pH-dependent growth rate increase compared to NRC-1. Growth medium consisted of CM⁺ buffered at (A) pH 6.1 with 100 mM PIPES; (B) pH 6.3 with 100 mM PIPES; (C) pH 7.2 with 100 mM MOPS; or (D) pH 7.5 with 100 mM MOPS. Representative curves of three replicates are shown. For J3-1 and NRC-1, the OD₆₀₀ values at 144 h were compared by two-tailed t-test. At pH 6.1, $P = 0.002$; at pH 6.3, $P = 0.01$; at pH 7.2, $P = 0.91$; at pH 7.5, $P = 0.45$. “*” indicates significant endpoint growth increase from NRC-1 ancestor in at least 2 replicates.

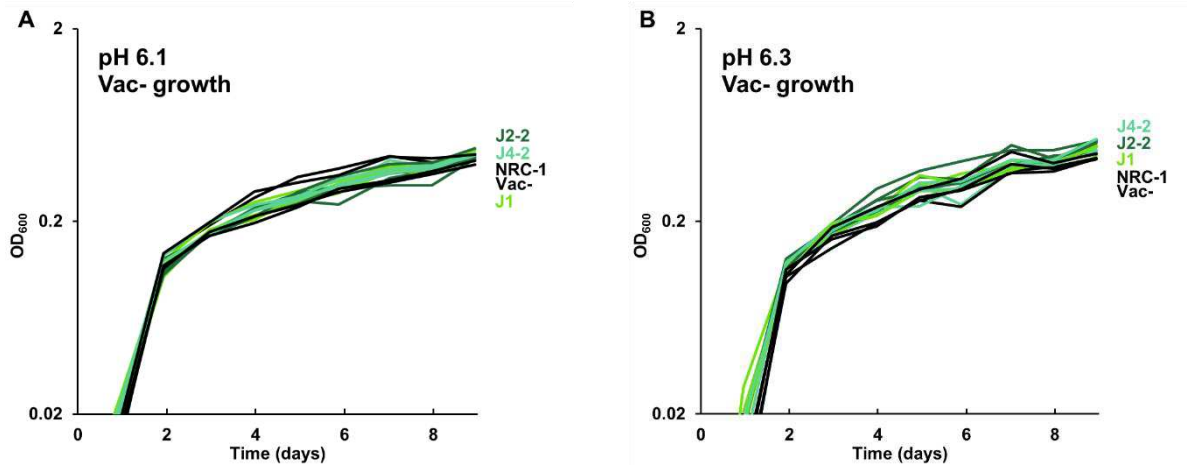


Figure 2. Growth of acid-evolved clones J1, J2-2, J4-2. Growth medium consisted of CM⁺ pH 6.3 with 100 mM PIPES, at (A) pH 6.1, (B) pH 6.3. Cultures were diluted from a 7-day culture in CM⁺ pH 7.2. Gas vesicle-deficient clones were compared to gas vesicle-deficient ancestral mutant NRC-1 and cell density values post log-phase (OD₆₀₀ at 6 days) were analyzed using ANOVA with Tukey post-hoc. Representative curves of three replicates are shown.

REFERENCES

1. Oren A. Life at high salt concentrations, intracellular KCl concentrations, and acidic proteomes. *Front Microbiol.* 2013;4(NOV):1–6.
2. Reysenbach A, Pace NR. *Archaea: A laboratory manual - Halophiles.* DasSarma S, Fleischmann E, editors. Cold Spring Harbor: Cold Spring Harbor Laboratory Press; 1995.
3. Ng W V., Kennedy SP, Mahairas GG, Berquist B, Pan M, Shukla HD, et al. Genome sequence of *Halobacterium* species NRC-1. *Proc Natl Acad Sci [Internet].* 2000;97(22):12176–81. Available from: <http://www.pnas.org/cgi/doi/10.1073/pnas.190337797>
4. Kish A, Kirkali G, Robinson C, Rosenblatt R, Jaruga P, Dizdaroglu M, et al. Salt shield: Intracellular salts provide cellular protection against ionizing radiation in the halophilic archaeon, *Halobacterium salinarum* NRC-1. *Environ Microbiol.* 2009;11(5):1066–78.
5. Jones DL, Baxter BK. DNA repair and photoprotection: Mechanisms of overcoming environmental ultraviolet radiation exposure in halophilic archaea. *Front Microbiol.* 2017;8:1882.
6. Coker JA, DasSarma P, Kumar J, Müller JA, DasSarma S. Transcriptional profiling of the model archaeon *Halobacterium* sp. NRC-I: Responses to changes in salinity and temperature. *Saline Systems.* 2007;3:doi:10.1186/1746-1448-3-6.
7. Wang G, Kennedy SP, Fasiludeen S, Rensing C, DasSarma S. Arsenic resistance in *Halobacterium* sp. strain NRC-1 examined by using an improved gene knockout system. *J Bacteriol [Internet].* 2004;186(10):3187–94. Available from: <http://www.ncbi.nlm.nih.gov/pubmed/15126481> <http://www.pubmedcentral.nih.gov/articlerender.fcgi?artid=PMC400623>
8. DasSarma P, Laye VJ, Harvey J, Reid C, Shultz J, Yarborough A, et al. Survival of halophilic archaea in Earth's cold stratosphere. *Int J Astrobiol.* 2017;16(4):321–7.
9. DasSarma P, DasSarma S. Survival of microbes in Earth's stratosphere. *Curr Opin Microbiol.* 2018;43:24–30.
10. DasSarma P, Tuel K, Nierenberg SD, Phillips T, Pecher WT, Nrc- H, et al. Inquiry-driven teaching & learning using the archaeal microorganism *Halobacterium*. *Am Biol Teach [Internet].* 2016;78(1):7–13. Available from: <http://www.bioone.org/doi/pdf/10.1525/abt.2016.78.1.7>
11. DasSarma S. Extreme halophiles are models for astrobiology. *Microbe [Internet].* 2006;1(3):120–6. Available from: <https://www.asm.org/ccLibraryFiles/FILENAME/000000002127/znw00306000120.pdf>
12. Leuko S, Domingos C, Parpart A, Reitz G, Rettberg P. The survival and resistance of *Halobacterium salinarum* NRC-1, *Halococcus hamelinensis*, and *Halococcus morrhuae* to simulated outer space solar radiation. *Astrobiology.* 2015;15(11):987–97.
13. Madden MEE, Bodnar RJ, Rimstidt JD. Jarosite as an indicator of water- limited chemical weathering on Mars. *Nature [Internet].* 2004;431(August):821–3. Available from: <https://www.nature.com/articles/nature02971.pdf>
14. Pritchett BN, Elwood Madden ME, Madden AS. Jarosite dissolution rates and maximum lifetimes in high salinity brines: Implications for Earth and Mars. *Earth Planet Sci Lett.* 2014;391:67–8.
15. Dopson M, Ossandon FJ, Lövgren L, Holmes DS. Metal resistance or tolerance? Acidophiles confront high metal loads via both abiotic and biotic mechanisms. *Front*

- Microbiol. 2014;5(157):doi: 10.3389/fmicb.2014.00157.
16. Moran-Reyna A, Coker JA. The effects of extremes of pH on the growth and transcriptomic profiles of three haloarchaea. *F1000 Res.* 2014;3(168):1–15.
 17. Lenski RE, Travisano M. Dynamics of adaptation and diversification: A 10,000-generation experiment with bacterial populations. *Proc Natl Acad Sci U S A* [Internet]. 1994 Jul 19 [cited 2015 Sep 9];91(15):6808–14. Available from: <http://www.pubmedcentral.nih.gov/articlerender.fcgi?artid=44287&tool=pmcentrez&rendertype=abstract>
 18. Lenski RE, Rose MR, Simpson SC, Tadler SC. Long-term experimental evolution in *Escherichia coli*. I. Adaptation and divergence during 2,000 generations. *Am Nat.* 1991;138:1315–41.
 19. Tenaillon O, Barrick JE, Ribeck N, Deatherage DE, Blanchard JL, Dasgupta A, et al. Tempo and mode of genome evolution in a 50,000 - generation experiment. *Nature* [Internet]. 2016;536(7615):165–70. Available from: <http://dx.doi.org/10.1038/nature18959>
 20. Creamer KE, Ditmars FS, Basting PJ, Kunka KS, Hamdallah IN, Bush SP, et al. Benzoate- and salicylate-tolerant strains of *Escherichia coli* K-12 lose antibiotic resistance during laboratory evolution. *Appl Environ Microbiol.* 2017;83(2):e02736.
 21. He A, Penix SR, Basting PJ, Griffith JM, Creamer KE, Camperchioli D, et al. Acid evolution of *Escherichia coli* K-12 eliminates amino acid decarboxylases and reregulates catabolism. *Appl Environ Microbiol.* 2017;83:e00442-17.
 22. Harden MM, He A, Creamer K, Clark MW, Hamdallah I, Martinez KA, et al. Acid-adapted strains of *Escherichia coli* K-12 obtained by experimental evolution. Schottel JL, editor. *Appl Environ Microbiol* [Internet]. 2015 Mar 15 [cited 2015 Sep 17];81(6):1932–41. Available from: <http://www.pubmedcentral.nih.gov/articlerender.fcgi?artid=4345379&tool=pmcentrez&rendertype=abstract>
 23. Schou MF, Kristensen TN, Kellermann V, Schlötterer C, Loeschcke V. A *Drosophila* laboratory evolution experiment points to low evolutionary potential under increased temperatures likely to be experienced in the future. *J Evol Biol.* 2014;27(9):1859–68.
 24. Slonczewski JL, Fujisawa M, Dopson M, Krulwich TA. Cytoplasmic pH measurement and homeostasis in bacteria and archaea. In: *Advances in Microbial Physiology.* 2009. p. 1–79, 317.
 25. Kanjee U, Houry WA. Mechanisms of acid resistance in *Escherichia coli*. *Annu Rev Microbiol.* 2013;67:65–81.
 26. Moore JP, Li H, Engmann ML, Bischof KM, Kunka KS, Harris ME, et al. Benzoate-tolerant *Escherichia coli* strains from experimental evolution lose the Gad regulon, multi-drug efflux pumps, and hydrogenases. *Appl Environ Microbiol.* 2019;
 27. Hamdallah I, Torok N, Bischof KM, Majdalani N, Chadalavada S, Mdluli N, et al. Experimental evolution of *Escherichia coli* K-12 at high pH and RpoS induction. *Appl Environ Microbiol.* 2018;84(13):e00520.
 28. DeVaux LC, Müller JA, Smith J, Petrisko J, Wells DP, DasSarma S. Extremely radiation-resistant mutants of a halophilic archaeon with increased single-stranded DNA-binding protein (RPA) gene expression. *Radiat Res.* 2007;168(4):507–14.
 29. McCarthy S, Johnson T, Pavlik BJ, Payne S, Schackwitz W, Martin J, et al. Expanding the limits of thermoacidophily in the archaeon *Sulfolobus solfataricus* by adaptive evolution.

- Appl Environ Microbiol. 2016;82(3):857–67.
30. Ai C, McCarthy S, Eckrich V, Rudrappa D, Qiu G, Blum P. Increased acid resistance of the archaeon, *Metallosphaera sedula* by adaptive laboratory evolution. J Ind Microbiol Biotechnol. 2016;43(10):1455–65.
 31. Dong Y, Chen YYM, Burne RA. Control of Expression of the Arginine Deiminase Operon of *Streptococcus gordonii* by CcpA and Flp. J Bacteriol. 2004;
 32. Sakanaka A, Kuboniwa M, Takeuchi H, Hashino E, Amano A. Arginine-ornithine antiporter ArcD controls arginine metabolism and interspecies biofilm development of *Streptococcus gordonii*. J Biol Chem. 2015;
 33. Krulwich TA, Sachs G, Padan E. Molecular aspects of bacterial pH sensing and homeostasis. Nat Rev Microbiol [Internet]. 2011;9:330–43. Available from: <http://dx.doi.org/10.1038/nrmicro2549>
 34. Lund P, Tramonti A, De Biase D. Coping with low pH: Molecular strategies in neutrophilic bacteria. FEMS Microbiol Rev. 2014;38(6):1091–125.
 35. Simsek M, DasSarma S, RajBhandary U, Khorana H. A transposable element from *Halobacterium halobium* which inactivates the bacteriorhodopsin gene. Proc Natl Acad Sci. 2006;79(23):7268–72.
 36. Dummer AM, Bonsall JC, Cihla JB, Lawry SM, Johnson GC, Peck RF. Bacterioopsin-mediated regulation of bacterioruberin biosynthesis in *Halobacterium salinarum*. J Bacteriol. 2011;193(20):5658–67.
 37. Ng W V., Ciufo SA, Smith TM, Bumgarner RE, Baskin D, Faust J, et al. Snapshot of a large dynamic replicon in a halophilic archaeon: Megaplasmid or minichromosome? Genome Res. 1998;8:1131–41.
 38. DasSarma S. Mechanisms of genetic variability in *Halobacterium halobium*: The purple membrane and gas vesicle mutations. Can J Microbiol. 1989;35(1):65–72.
 39. Sapienza C, Doolittle WF. Unusual physical organization of the *Halobacterium* genome. Nature. 1982;295(5848):384–9.
 40. Wimmer F, Oberwinkler T, Bisle B, Tittor J, Oesterhelt D. Identification of the arginine/ornithine antiporter ArcD from *Halobacterium salinarum*. FEBS Lett. 2008;582:3771–5.
 41. Ruepp A, Soppa J. Fermentative arginine degradation in *Halobacterium salinarum* (formerly *Halobacterium halobium*): Genes, gene products, and transcripts of the *arcRACB* gene cluster. J Bacteriol. 1996;178(16):4942–7.
 42. Deatherage DE, Barrick JE. Identification of mutations in laboratory-evolved microbes from next-generation sequencing data using *breseq*. Sun L, Shou W, editors. Methods Mol Biol [Internet]. 2014;1151:165–88. Available from: <http://link.springer.com/10.1007/978-1-4939-0554-6>
 43. Deatherage DE, Traverse CC, Wolf LN, Barrick JE. Detecting rare structural variation in evolving microbial populations from new sequence junctions using *breseq*. Front Genet. 2015;5(JAN):1–16.
 44. Barrick JE, Colburn G, Deatherage DE, Traverse CC, Strand MD, Borges JJ, et al. Identifying structural variation in haploid microbial genomes from short-read resequencing data using *breseq*. BMC Genomics. 2014;15(1):1039.
 45. Pfeiffer F, Schuster SC, Broicher A, Falb M, Palm P, Rodewald K, et al. Evolution in the laboratory: The genome of *Halobacterium salinarum* strain R1 compared to that of strain NRC-1. Genomics. 2008;91(4):335–46.

46. Pfeiffer F, Marchfelder A, Habermann B, Dyall-Smith ML. The Genome Sequence of the *Halobacterium salinarum* Type Strain Is Closely Related to That of Laboratory Strains NRC-1 and R1. *Microbiol Resour Announc*. 2019;
47. DasSarma S, Halladay JT, Jones JG, Donovan JW, Giannasca PJ, de Marsac NT. High-frequency mutations in a plasmid-encoded gas vesicle gene in *Halobacterium halobium*. *Proc Natl Acad Sci U S A* [Internet]. 1988;85(18):6861–5. Available from: <http://www.pubmedcentral.nih.gov/articlerender.fcgi?artid=282078&tool=pmcentrez&rendertype=abstract>
48. Ng W, DasSarma S. Physical and genetic mapping of the unstable gas vesicle plasmid in *Halobacterium halobium* NRC-1. In: Rodriguez-Valera F, editor. *General and Applied Aspects of Halophilic Microorganisms*. Plenum Press; 1991. p. 305–11.
49. Ng WL, Kothakota S, DasSarma S. Structure of the gas vesicle plasmid in *Halobacterium halobium*: Inversion isomers, inverted repeats, and insertion sequences. *J Bacteriol*. 1991;173:1958–64.
50. Ng WL, Arora P, DasSarma S. Large deletions in class III gas vesicle-deficient mutants of *Halobacterium halobium*. *Syst Appl Microbiol*. 1993;16:560–8.
51. Soppa J. Evolutionary advantages of polyploidy in halophilic archaea. *Biochem Soc Trans*. 2013;41(1):339–43.
52. Gong S, Richard H, Foster JW. YjdE (AdiC) is the arginine:agmatine antiporter essential for arginine-dependent acid resistance in *Escherichia coli*. *J Bacteriol*. 2003;185(15):4402–9.
53. DasSarma S, Arora P. Genetic analysis of the gas vesicle gene cluster in haloarchaea. *FEMS Microbiol Lett*. 1997;153(1):1–10.
54. DasSarma P, Zamora RC, Müller JA, DasSarma S. Genome-wide responses of the model archaeon *Halobacterium* sp. strain NRC-1 to oxygen limitation. *J Bacteriol*. 2012;194(20):5530–7.
55. DasSarma S, Arora P, Lin F, Molinari E, Yin LRS. Wild-type gas vesicle formation requires at least ten genes in the *gvp* gene cluster of *Halobacterium halobium* plasmid pNRC100. *J Bacteriol*. 1994;176(24):7646–52.
56. Nelson-Sathi S, Dagan T, Landan G, Janssen A, Steel M, McInerney JO, et al. Acquisition of 1,000 eubacterial genes physiologically transformed a methanogen at the origin of Haloarchaea. *Proc Natl Acad Sci*. 2012;109(50):20537–42.
57. Redder P, Garrett RA. Mutations and rearrangements in the genome of *Sulfolobus solfataricus* P2. *J Bacteriol*. 2006;188(12):4198–206.
58. Griffith JM, Basting PJ, Bischof KM, Wrona EP, Kunka KS, Tancredi A, et al. Experimental evolution of *Escherichia coli* K-12 in the presence of proton motive force (PMF) uncoupler carbonyl cyanide m-chlorophenylhydrazone selects for mutations affecting PMF-driven drug efflux pumps. *Appl Environ Microbiol*. 2019;85(5):e02792-18.
59. Berquist BR, Müller JA, DasSarma S. 27 genetic systems for halophilic archaea. *Methods Microbiol*. 2006;35:649–80.
60. Thorvaldsdóttir H, Robinson JT, Mesirov JP, Thorvaldsdóttir H, Robinson JT, Mesirov JP. Integrative genomics viewer (IGV): High-performance genomics data visualization and exploration. *Brief Bioinform*. 2013;14(2):178–92.

DECLARATIONS**Ethics approval and consent to participate**

Not Applicable

Consent for publication

Not Applicable

Availability of data and materials

Sequenced genomes are deposited at NCBI under SRA accession number SRP195828.

<https://www.ncbi.nlm.nih.gov/sra/SRP195828>

Competing interests

The authors declare that they have no competing interests.

Funding

This project was supported by the National Science Foundation award MCB-1613278 to Joan Slonczewski; by the 2016 NASA Astrobiology Program Early Career Collaboration Award to Karina Kunka and Jessie Griffith; and by NASA Exobiology grants NNX15AM07G and NNH18ZDA001N to Shiladitya DasSarma.

Authors' contributions

KSK designed the study, performed most of the experiments, and drafted the manuscript. JMG co-designed the study and performed many of the experiments. CH conducted growth curves and analyzed resequenced genomes. KMB conducted growth curves and analyzed genomes. HL conducted growth curves. PD advised and trained students on haloarchaea procedures. SD mentored and trained students, and contributed to study design. JLS conceived the central concept, mentored students, and completed the manuscript.

Acknowledgements

We thank Friedhelm Pfeiffer for pointing out the arcD annotation. We thank Landon Porter for expert technical assistance.

Figures

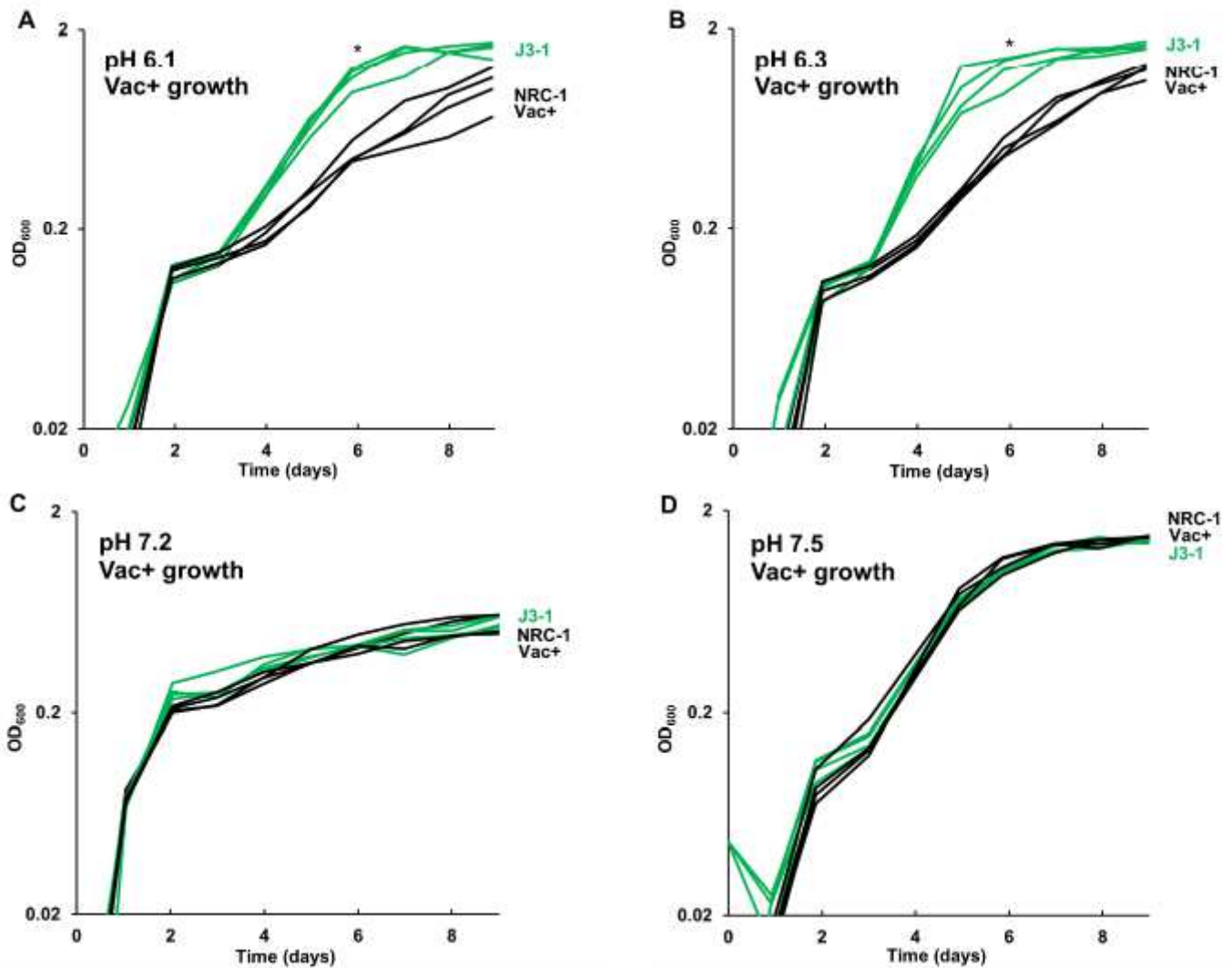


Figure 1

Acid-evolved clone J3-1 shows a pH-dependent growth rate increase compared to NRC-1. Growth medium consisted of CM+ buffered at (A) pH 6.1 with 100 mM PIPES; (B) pH 6.3 with 100 mM PIPES; (C) pH 7.2 with 100 mM MOPS; or (D) pH 7.5 with 100 mM MOPS. Representative curves of three replicates are shown. For J3-1 and NRC-1, the OD₆₀₀ values at 144 h were compared by two-tailed t-test. At pH 6.1, $P = 0.002$; at pH 6.3, $P = 0.01$; at pH 7.2, $P = 0.91$; at pH 7.5, $P = 0.45$. “*” indicates significant endpoint growth increase from NRC-1 ancestor in at least 2 replicates.

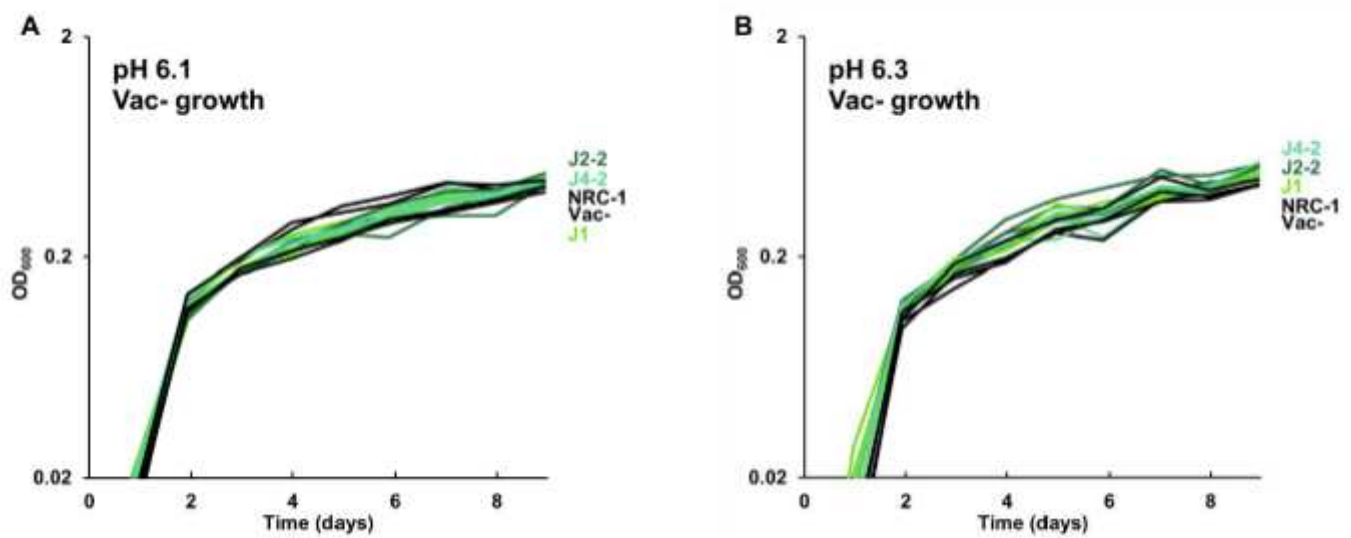


Figure 2

Growth of acid-evolved clones J1, J2-2, J4-2. Growth medium consisted of CM+ pH 6.3 with 100 mM PIPES, at (A) pH 6.1, (B) pH 6.3. Cultures were diluted from a 7-day culture in CM+ pH 7.2. Gas vesicle-deficient clones were compared to gas vesicle-deficient ancestral mutant NRC-1 and cell density values post log-phase (OD₆₀₀ at 6 days) were analyzed using ANOVA with Tukey post-hoc. Representative curves of three replicates are shown.

Supplementary Files

This is a list of supplementary files associated with this preprint. Click to download.

- [HaloAdditionalFile1Rev2.xlsx](#)